URSI GASS 2020, Rome, Italy, 29 August - 5 September 2020

The simulation of powerful high-frequency induced parametric decay instability and oscillation two stream instability in ionosphere

M. Liu(1), C. Zhou* (1), and T. Feng(1)
(1) School of Electronic Information, Wuhan University, Wuhan, China, 430072

Abstract

We present a two-fluid simulation of the interaction between the powerful HF (high-frequency) electromagnetic wave and the ionosphere. The OTSI (Oscillation Two-Stream Instability) and PDI (Parametric Decay Instability), near and below the turning point of ordinary wave mode respectively, are excited. The region of coexistence of OTSI and PDI is investigated. The spectral features in OTSI, PDI and coexistence area are studied. The wave conversion from O mode to Z mode is studied by using different source intensity.

1 Introduction

The HF-induced plasma line and ion line has been observed in many ionospheric radio modification experiments [1-4]. The PPI (Ponderomotive Parametric Instability) theory, include PDI, OTSI and other parametric instability induced by Ponderomotive force, is followed to interpret the spectral features [5-7]. In PDI process, the pump wave (ω_0, $\boldsymbol{k_0}$) decays into a Langmuir wave (ω_L, $\boldsymbol{k_L}$) and an ion acoustic wave (ω_{IA}, $\boldsymbol{k_{IA}}$), where the phase matching conditions $\omega_0=\omega_L+\omega_{IA}$, $\boldsymbol{k_0= k_L+ k_{IA}}$ are satisfied. The Langmuir wave can further decay into a daughter Langmuir wave and an acoustic wave, which is described by cascade theory, also known as WTA (weak Langmuir turbulence approximation). The OTSI process involves the decay of pump wave to two Langmuir sidebands and a purely growing mode, which is corresponding with cavitons formation [8-11].

The numerical simulations of PDI have been reported in many studies [12-14], while simulation about OTSI is present mostly in SLT study [8-11]. Both two processes simulation are almost based on Zakharov model. In this study, more general equations are computed to simulate both OTSI and PDI under different intensity of electric field and the spectral feature are analyzed. Conversion from O mode to Z mode with the intensity of electric field is studied.

2 Numerical Model

To numerically simulate the radio wave propagation in the ionosphere, the curl Maxwell equations (1) are computed by FDTD (Finite-Difference Time-Domain) scheme,

$$\begin{cases} \nabla\times\vec{E}=-\mu_0\dfrac{\partial\vec{H}}{\partial t} \\ \nabla\times\vec{H}-\vec{J}=-\mu_0\dfrac{\partial\vec{H}}{\partial t} \end{cases} \tag{1}$$

where $\vec{J}$ is the current from the dynamics of electrons and ions. In this paper, the O^+ is considered for ions. The dynamics of electrons and ions are governed by equation (2) and (3), where n is the density, v is velocity, m is the mass, z is the vertical spatial coordinate, subscript e and i represent electrons and ions, $v_{Te}=(k_BT_e/m_e)^{1/2}$ is the electron thermal speed and $C_s=[k_B(T_e+3T_i)/m_i]^{1/2}$ is the ion acoustic speed, k_B is Boltzmann's constant, T_e and T_i are temperature of electrons and ions. The Ponderomotive force is considered in the ion momentum equation. Constant geomagnetic field B_0 is considered. The density fluctuations are separated into fast and slow timescale. So we define the electron density $n_e=n_{e0}+n_{es}+n_{eh}$, where n_{e0} is the background electron density, n_{es} is the fluctuation in slow timescale and n_{eh} is the fluctuation in fast timescale. Similarly, the ion density is defined by $n_i=n_{i0}+n_{is}+n_{ih}$. Here quasi-neutrality is assumed in background electron density and slow timescale, i.e. $n_{e0}=n_{i0}=n_0$ and $n_{es}=n_{is}=n_s$. The ion fluctuation in fast timescale is zero, namely $n_{ih}=0$, which means that ions are assumed to be immobile in high-frequency process.

$$\begin{cases} \dfrac{\partial n_{eh}}{\partial t}=-\dfrac{\partial(n_{es}+n_{e0})v_{ez}}{\partial z} \\ \dfrac{\partial\vec{v}_e}{\partial t}=-\dfrac{\mathrm{e}}{m_e}[\vec{E}+\vec{v}_e\times\vec{B}_0]-\dfrac{3v_{Te}^2}{n_\mathrm{e}}\dfrac{\partial n_e}{\partial z}\vec{z}-\upsilon_e\vec{v}_e \end{cases} \tag{2}$$

$$\begin{cases} \dfrac{\partial n_{is}}{\partial t}=-n_0\dfrac{\partial v_i}{\partial z} \\ \dfrac{\partial v_i}{\partial t}=-C_s{}^2\dfrac{\partial n_i}{\partial z}-\upsilon_i v_i-\dfrac{1}{4}\dfrac{\mathrm{e}^2}{m_i m_e\omega_0^2}\dfrac{\partial\left|E_h\right|^2}{\partial z} \end{cases} \tag{3}$$

3 Numerical Setup

The computation of above numerical model is accelerated by GPU. A computational domain of dimensions 86538×1 Yee cells [15] is used, with the spatial step size set as 0.04 m, which means that total computation height range is 0 – 3461.52 m. The boundaries on both sides are 256 cell PML (Perfect-Matched-Layer) boundaries [16]. The background electron density profile n_0 is assumed to have a Gaussian shape as formula (4).

$$n_0(z) = n_{max} exp\left[-(z - z_{max})^2 / L^2\right] \quad (4)$$

where n_{max} =1.436×10^{11} m^{-3} is the electron density at the F2 peak located at z_{max}= 13.418 km, which height is beyond the computation domain, and L=31.62 km is the ionosphere scale length. The pump frequency is chosen as f_0=3.2 MHz, from which the turning point of O mode wave can be calculated as z_0=2.352 km. The source electromagnetic wave is at z=0 km and pump wave is set as O mode. The temperature of electrons and ions are both chosen as 1500 K. The geomagnetic field is set to the case at the EISCAT facility in Tromso as

$$\vec{B} = B_0[\vec{x}\sin(\theta) - \vec{z}\sin(\theta)] \quad (5)$$

where θ = 12°, B_0 is set as typical value B_0 =5×10^{-5} T.

4 Simulation Results

We compare the simulation in different pump intensity. Firstly, the pump intensity E_0=1 V/m is chosen, which is so large that induce a PPI in broad height range. Fig 1 shows the evolution of the z-direction electric field E_z and ions density change n_s. Large scale standing wave is formed soon due to the reflection after simulation start. At about t=4 ms, the small scale structures are generated significantly around z=2.4 km, 1.9 km and 1.8 km, which demonstrates that PPI is excited. Meanwhile, standing wave at z=2.4 km moves down and become more intensive, which seems to be compressed by the small scale structure. In addition, new wave above turning point of O mode is generated and propagation upwards, which mean the Z mode wave is converted due to the small scale structure. After then, small structure is generated at lower height with time because of the lower intensity of standing wave at lower height.

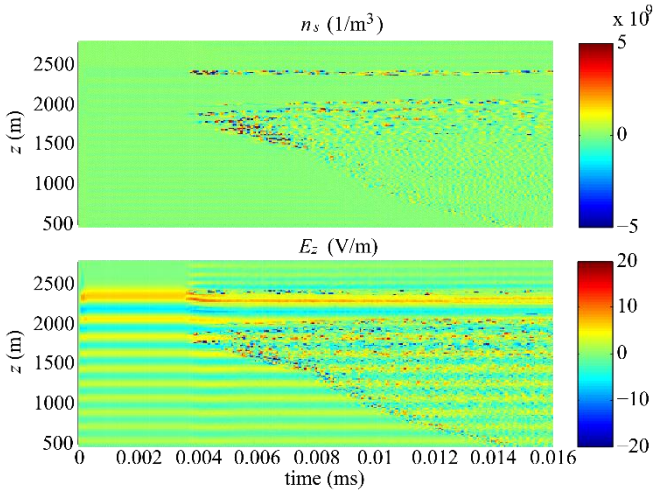

Figure 1. The evolution of z-direction field E_z and ion density change n_s.

To distinguish the PDI and OTSI in Figure 1, the spectrum of ion density change with height is showed, as Figure 2. Below the height of z=1580 m, two discrete spectrum enhancement is obvious, and the relationship between the two frequencies is exactly double, which is consistent with cascade theory. The spectrum above z=1580 m is enhanced at zero frequency, which is the OTSI spectral feature.

Based on dispersion relation of Langmuir wave as equation (6),

$$\omega_L^2 = \omega_p^2 + 3\boldsymbol{k}_L v_{Te}^2 + \omega_{ce}^2 \sin^2\theta \quad (6)$$

and ion acoustic wave as equation (7)

$$\omega_{IA} = |\boldsymbol{k}_{IA}| C_s \quad (7)$$

and match condition, where ω_{ce} is the electrons gyro-frequency, the prediction about the acoustic wave frequency of primary PDI is present as equation (8), which is computed with our simulation parameters and plotted in Figure 2 as black line. The black line fit the enhanced spectrum by primary decay process in Figure 2 pretty well. The predicted acoustic frequency gets lower with height from equation (8), i.e., the black line in Figure 2. Let $|f_{IA}|$=0, the height can be calculated as $z_{p,max}$= 2119.48 m. The height $z_{p,max}$ represents the maximum height where PDI can be excited. So, in figure 2, the PPI excited around z=2400 m should be only OTSI process. Between z=1580 m-2050m, both PDI and OTSI processes are excited.

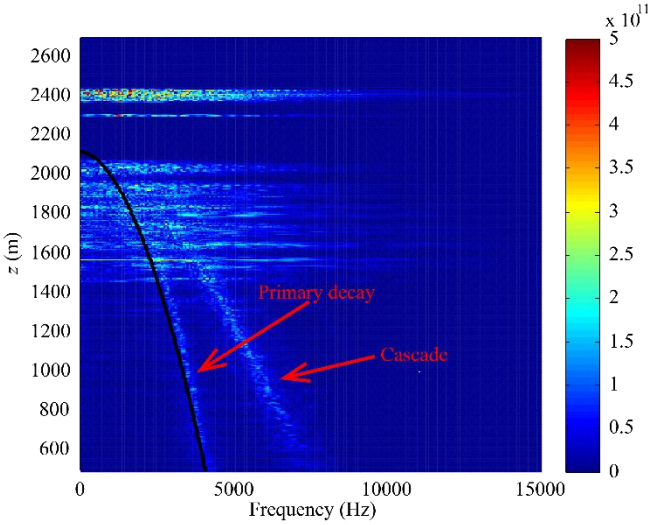

Figure 2. The ion density change n_s frequency spectrum with height. The black line is the prediction of ion acoustic wave frequency induced by primary PDI from equation (8).

$$\begin{cases} |k_{IA}| = \dfrac{-2\omega_0 C_s + 2\sqrt{(C_s^2 - 3v_{Te}^2)\times(\omega_p^2 - \omega_{ce}^2\sin^2(\theta)) + 3v_{Te}^2\omega_0^2}}{2(3v_{Te}^2 - C_s^2)} \\ f_{IA} = \dfrac{|k_{IA}| C_s}{2\pi} \end{cases} \quad (8)$$

Figure 3 shows the evolution of n_s at three different regions, where only OTSI is excited, both OTSI and PDI excited, and only PDI is excited. The cavitons are observed at upper panel and middle panel. The propagation of cavitons can be observed too, which is corresponding with the collapse and nucleation of cavitons. The depth of cavitons between 2386 m – 2393 m is larger than that between 1706 m -1713 m, because of the intensity of standing wave as pump wave is larger

between 2386 m – 2393 m. The *f-k* spectrum at these three regions are present in Figure 4, where the trace of enhanced spectrum in three panels are all consistent with acoustic wave dispersion relation. However, the differences between three panels should be mentioned. The significantly discrete spectral feature at bottom panel, consistent with cascade theory [11], also demonstrates the PDI and cascade are excited. In the middle panel and upper panel, the spectrum is broad and continuous, which is derived from the collapse. But the maximum enhancement can be observed at k_0=1 m^{-1} and k =N k_0 at middle panel, where N is an integer. This spectral feature may come from the harmonic wave number of formation of cavitons. At upper panel, the harmonic enhancement of cavitons are invisible. It may be covered by the spectrum extension due to violent collapse.

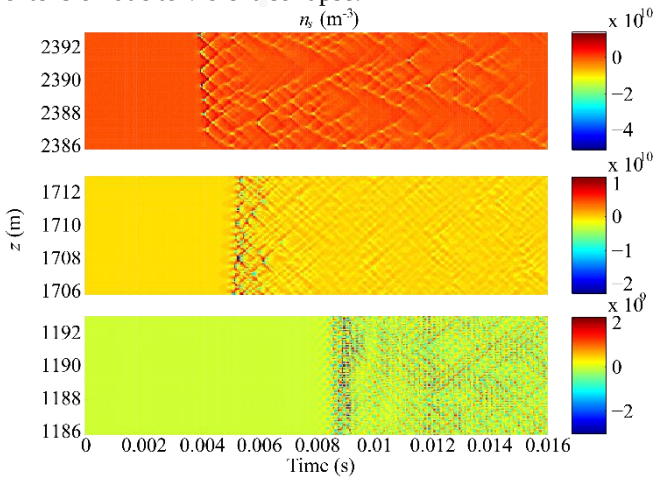

Figure 3. The ion density change n_s at three different regions.

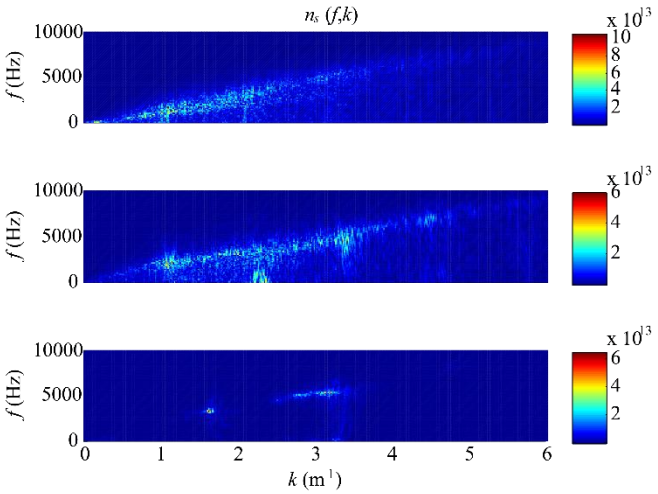

Figure 4. The *f-k* spectrum at these three regions corresponding with Figure 3.

Next the intensity of source is changed to be 0.8 V/m, in which case the OTSI at z=2400 m is not excited. Ion density change n_s frequency spectrum with height are showed as Figure 5. The OTSI is not most easily excited in reflection height, because the threshold of OTSI get greater while the height is closer to the reflection height [17]. The height range where both PDI and OTSI are excited are slightly narrowed.

The conversion from O mode to Z mode wave due to cavitons is studied. The simulation is run with eight different source intensity E_0. Here the conversion ratio is defined as the ratio of maximum electric field between z=2800 m – 3200 m after small scale structure generation to maximum standing wave intensity before small scale structure generation. The result is plotted as Figure 6. The red star represents the OTSI at=2400 m is excited. The black star represents the OTSI at z=2400 m is not excited and in these situation the maximum height of small scale structure generation is about z=2100 m. The conversion rate gets larger with source intensity. The more important factor to be considered is the height of cavitons. The dispersion relation curves of O mode and Z mode are closer near reflection height than that far below the reflection height, which induced more effective conversion while OTSI near reflection height is excited and cavitons are generated.

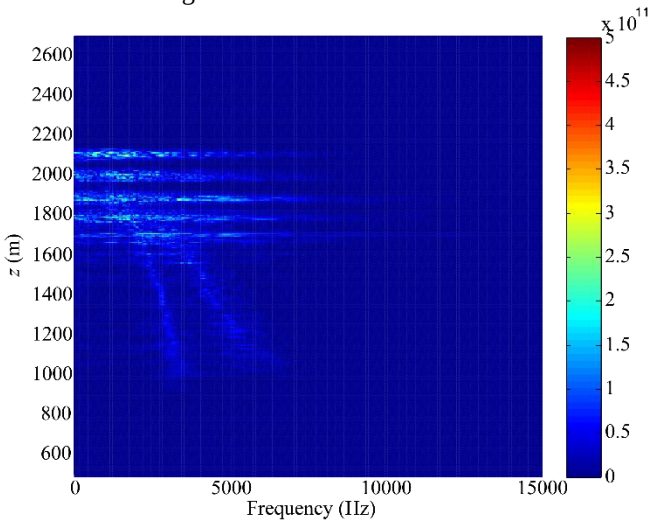

Figure 5. Same as Figure 2 but source intensity E_0=0.8 V/m.

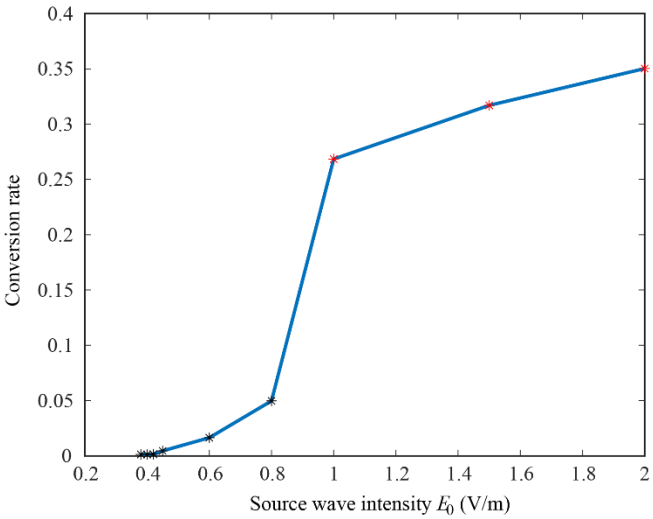

Figure 6. The Conversion rate from O mode to Z mode with source intensity E_0.

5 Summary

Two-fluid model is numerally simulated in this study. The OTSI and PDI process are excited in the simulation. The cycle of nucleation, collapse of cavitons are observed in OTIS process, which is corresponding with the propagation of cavitons. The cascade is observed in PDI process.

The region of OTSI excitation is higher than that of PDI, which is consistent with the previous studies. At the junction, two process are coexistent. The height range of coexistence depends on the power of source.

The spectral feature in different region is studied. The PDI excitation shows a discrete spectrum. Prediction of ion acoustic wave frequency in primary PDI is present, which is consistent with the simulation pretty well. The spectrum enhancement is broad and continuous in OTSI due to the formation and collapse of cavitons. In existence region, the spectrum is same as OTSI area except the harmonic wave enhancement.

The conversion from O mode to Z mode is studied by the simulations in different source intensity. The maximum height of cavitons generation is important. The closer the cavitons gets to the reflection height, the conversion is more effective. The source intensity can also influence the conversion by influencing the cavitons depth.

6 References

1. H. C. Carlson, W. E. Gordon, and R. L. Showen, "High frequency induced enhancements of the incoherent scatter spectrum at Arecibo," *J. Geophys. Res*., **77**, 7, March 1972, pp.1242-1250, doi:10.1029/JA077i007p01242.

2. J. A. Fejer, "Ionospheric modification and parametric instabilities," *Reviews of Geophysics*, **17**, 1, February 1979, pp. 135-153, doi:10.1029/RG017i001p00135.

3. A. Westman, T. B. Leyser, G. Wannberg, and M. T. Rietveld, "Tristatic EISCAT-UHF measurements of the HF modified ionosphere for low background electron temperature," *J. Geophys. Res*., **100,** A6, June 1995, pp. 9717-9728, doi:10.1029/94JA03337.

4. T. Hagfors, W. Kofman, H. Kopka, and T. Äijanen, "Observations of enhanced plasma lines by EISCAT during heating experiments," *Radio Science*, **18**, 06, December 1983, pp, 861-866, doi:10.1029/RS018i006p00861.

5. W. L. Kruer, and E. J. Valeo. "Nonlinear evolution of the decay instability in a plasma with comparable electron and ion temperatures," *The Physics of Fluids*, **16**, 675, 1973, pp. 675-682, doi:10.1063/1.1694402.

6. J. A. Fejer, and Y. Y. Kuo, "Structure in the nonlinear saturation spectrum of parametric instabilities," *The Physics of Fluids*, **16**, 9, 1973, pp.1490-1496, doi:10.1063/1.1694546.

7. F. W. Perkins, C. Oberman, E. J. Valeo, "Parametric instabilities and ionospheric modification," *J. Geophys. Res*., **79**, 10, April 1974, pp.1478-1496, doi: 10.1029/JA079i010p01478.

8. G. D. Doolen, D. F. DuBois, and H. A. Rose, "Nucleation of cavitons in strong Langmuir turbulence," *Phys. Rev. Lett.*, **54**, 8, February 1985, pp.804-807, doi:10.1103/PhysRevLett.54.804.

9. D. Russell, D. F. DuBois, and H. A. Rose, "Nucleation in two dimensional Langmuir turbulence," *Phys. Rev. Lett.*, **60**, 7, February 1988, pp.581-584, doi:10.1103/PhysRevLett.60.581.

10. D. F. DuBois, H. A. Rose, and D. Russell, "Coexistence of parametric decay cascades and caviton collapse at subcritical densities", *Phys. Rev. Lett.*, **66**, 15, April 1991, pp.1970-1973, doi:10.1103/PhysRevLett.66.1970.

11. Alfred Hanssen, E. Mjølhus, D. F. DuBois, and H. A. Rose, "Numerical test of the weak turbulence approximation to ionospheric Langmuir turbulence," *J. Geophys. Res*., **97**, A8, August 1992, pp.12073-12091, doi: 10.1029/92JA00874.

12. N. R. Pereira, R. N. Sudan, and J. Denavit, "Numerical study of two-dimensional generation and collapse of Langmuir solitons," *The Physics of Fluids*, **20**, 6, 1977, pp. 936-945, doi:10.1063/1.861981.

13. B. Eliasson, and L. Stenflo, "Full-scale simulation study of the initial stage of ionospheric turbulence," *J. Geophys. Res*., **113**, A2, February 2008, doi:10.1029/2007JA012837.

14. T. J. Heelis, K. Ronald, and B. E. Eliasson, "Large-scale numerical simulation of ionospheric Langmuir turbulence excited by a radio frequency electromagnetic wave," *Plasma Physics and Controlled Fusion*, **61**, February 2019, doi:10.1088/1361-6587/aaf693.

15. K. S. Yee, "Numerical solution of initial boundary value problems involving maxwell's equations in isotropic media," *IEEE Trans. Antennas Propag.*, **14**, 3, May 1966, pp. 302-307, doi:10.1109/TAP.1966.1138693.

16. J. P. BERENGER, "A perfectly matched layer for the absorption of electromagnetic waves," *Journal of computational physics*, **114**, 2, October 1994, pp.185-200, doi:10.1006/jcph.1994.1159.

17. S. P. Kuo, "Oscillating two-stream instability in ionospheric heating experiments," *Physics of Plasmas*, **9**, 4, March 2002, pp. 1456-1459, doi:10.1063/1.1453471.